INVITED PAPER *Joint Special Section on Opto-electronics and Communications for Future Optical Network*

# Advantages of SOA Assisted Extended Reach EADFB Laser (AXEL) for Operation at Low Power and with Extended Transmission Reach

**Wataru KOBAYASHI**[†a)], **Naoki FUJIWARA**[††], **Takahiko SHINDO**[†], **Yoshitaka OHISO**[†], **Shigeru KANAZAWA**[††], ***Members***, **Hiroyuki ISHII**[†], ***Senior Member***, **Koichi HASEBE**[†], **Hideaki MATSUZAKI**[†], ***and*** **Mikitaka ITOH**[†], ***Members***

**SUMMARY** We propose a novel structure that can reduce the power consumption and extend the transmission distance of an electro-absorption modulator integrated with a DFB (EADFB) laser. To overcome the trade-off relationship of the optical loss and chirp parameter of the EA modulator, we integrate a semiconductor optical amplifier (SOA) with an EADFB laser. With the proposed SOA assisted extended reach EADFB laser (AXEL) structure, the LD and SOA sections are operated by an electrically connected input port. We describe a design for AXEL that optimizes the LD and SOA length ratio when their total operation current is 80 mA. By using the designed AXEL, the power consumption of a 10-Gbit/s, 1.55-$\mu$m EADFB laser is reduced by 1/2 and at the same time the transmission distance is extended from 80 to 100 km.

***key words:*** *electro-absorption modulator, semiconductor optical amplifier, DFB laser*

## 1. Introduction

The continuous increase in data traffic caused by the use of smart phones and cloud computing has resulted in increased power consumption at datacenters. This increase in power consumption is becoming a social issue, because it has a big impact on our total daily power consumption. There are two ways to reduce datacenter power consumption. One is to reduce the power consumption of the optical network system itself, and the other is to reduce the number of datacenter branches and thus eliminate the power needed for transmitting between datacenters. Although there are two effective approaches, they are both affected by the same bottleneck, namely the characteristics limitation of the optical devices that support optical network systems. The challenge now is to try to reduce the power consumption of the optical devices and increase their transmission distance, while simultaneously increasing the signaling rate.

An electroabsorption modulator integrated with a distributed feedback (EADFB) laser is widely used as an optical light source for many applications such as datacenter connection, and within datacenters. In fact, the EADFB laser has already been employed in a 100GbE optical system [1], and is expected to be employed in a 400GbE optical system [2]. We believe there is a strong need to reduce the power consumption of the EADFB laser and extend the transmission distance without any drawbacks. However, there is a technical issue with the EADFB laser as regards reducing its power consumption while simultaneously extending its transmission distance. The Kramers-Kronig (K-K) relation of the EA modulator (EAM) inevitably limits any simultaneous improvement of power consumption and transmission distance. This means that if we want to extend the available distance for the EAM, its optical loss inevitably increases. The LD injection current needs to be increased to compensate for this loss, and this results in increased power consumption. There have been some reports describing how to improve the characteristics of the EADFB laser by designing the multiple-quantum well (MQW) structure of the EAM section and optimizing the entire structure of the EADFB laser [3]–[7]. But optimization of the MQW cannot overcome the K-K relation, and therefore a novel approach is required.

There have been some reports about a new concept that could lead to a breakthrough allowing the EADFB laser to overcome the K-K relationship problem. A dual-modulation scheme has been reported [8]. This method can extend the transmission distance of the EAM, but it requires complicated phase tuning of the electrical input signal and an additional RF input port for the LD. A chirp compensation scheme with a semiconductor optical amplifier (SOA) has been reported [9]. This method can use a reverse change in carrier density for the EA and SOA sections, and this can suppress the chirp parameter of the EA section. An important problem with this scheme is how to suppress the additional power consumption needed for the SOA section compared with a conventional EADFB laser. Recently, we demonstrated an optical output power increase with reduced power consumption by integrating a short SOA with an EADFB laser [10]. We also demonstrated a method of suppressing the pattern effect of the SOA by changing the injection current of the SOA section [11]. These reports indicate that integrating a short SOA with an EADFB laser greatly improves the characteristics of the EADFB laser without any increase in total power consumption. The final goal is to re-

Manuscript received January 30, 2017.
Manuscript revised April 18, 2017.
[†]The authors are with NTT Device Technology Laboratories, NTT Corporation, Atsugi-shi, 243–0198 Japan.
[††]The authors are with NTT Device Innovation Center, NTT Corporation, Atsugi-shi, 243–0198 Japan.
a) E-mail: kobayashi.wataru@lab.ntt.co.jp
DOI: 10.1587/transele.E100.C.759

place the EADFB laser with an EADFB SOA, and an additional electrical input port must be removed. To solve this problem, we proposed a novel approach called an SOA assisted extended reach EADFB laser (AXEL) [12], [13], and this structure also provides improved characteristics with a conventional EADFB laser in spite of the electrical input port for the SOA section being removed. In this structure, the LD and SOA are electrically connected. We used an AXEL to investigate how the electrical connection of the LD and SOA affects the total power consumption in the 1.57-$\mu$m-wavelength window [14]. Because an AXEL can improve the launch power of the optical transmitter, we extend this concept to the 1.3 $\mu$m wavelength to increase the transmission link budget, and realized a 25-Gbit/s, 80 km SMF transmission compared with the conventional distance of 40 km [15].

In this paper, we propose the concept of the AXEL. We also describe a design method for this concept and explain the keys to designing this device. We confirm the advantages of the low power operation and extended transmission distance of our designed AXEL in actual use compared with the conventional EADFB laser at 10 Gbit/s in the 1.55-$\mu$m-wavelength window.

## 2. Concept

Figure 1 shows the concept of the AXEL. To overcome the limitation of the conventional EADFB laser, an SOA is integrated with an EADFB laser. SOA integration has two advantages. One is the amplified optical output power provided by the SOA with the same injection current as a conventional EADFB laser [12]. Generally the optical output power of a conventional EADFB laser is affected by the EAM optical loss. This means that some of the current injected into the LD section is used to compensate for the optical loss of the EAM. On the other hand, the optical output from the SOA is not affected by the EAM optical loss, because the SOA is close to an output facet of the device. When the LD and SOA are fabricated with the same MQW structure, the induced gain becomes roughly the near value. So the current efficiency to optical power ratio for an SOA is better than that of an LD in terms of EAM optical loss. For this reason, the optical output power of an AXEL is larger than that of a conventional EADFB laser as shown in Fig. 1. The other advantage of an AXEL is chirp compensation thanks to the SOA [9]. This is the result of the reversed carrier density change for the EAM and the SOA sections. As shown in Fig. 1, when the SOA is integrated with an EADFB laser, the sum of the LD and SOA lengths naturally exceeds the LD length, and therefore the electrical resistance of the LD and SOA sections for the AXEL is smaller than that of LD section of the EADFB laser, and this results in a reduction in the bias voltage for the LD section. In addition, when the SOA is integrated with an EADFB laser, the LD section current is reduced and the output power from the LD inevitably decreases. This results in a reduction in the photocurrent and power consumption ($P$) of the EAM.

On the other hand, there is one problem as regards SOA integration. That is, an additional electrical input port is needed for the SOA compared with the conventional EADFB laser. To overcome this problem and finally replace the EADFB laser with an EADFB laser integrated with an SOA, we propose a novel approach as shown in Fig. 1. The LD and SOA sections are electrically connected, and the injected current is automatically divided into each section according to their lengths. No additional electrical input port is needed to operate this device. From the point of view of the fabrication process, no additional epitaxial growth for the SOA section is required. We employed the same InGaAlAs core layer for the LD and SOA section. The InGaAlAs EA core layer is butt-jointed to the LD and SOA core layer. With the AXEL we can expect improved energy efficiency and transmission characteristics compared with the conventional EADFB laser without any drawbacks. In the next section, we describe the AXEL design method.

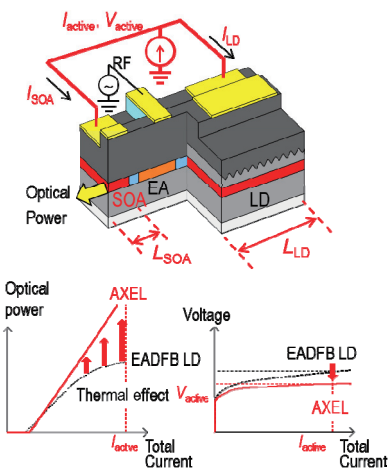


**Fig. 1** Concept of AXEL.

## 3. Design Methodology

In this section, we describe the design methodology we used for the AXEL. Figure 2 shows the AXEL calculation model and related assumptions. Since the LD section of the conventional EADFB laser is driven by an injection current ($I_{LD}$) of 80 mA [10], we set the sum of the injection currents

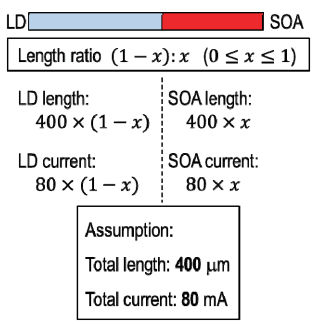


**Fig. 2** AXEL calculation model and assumptions.

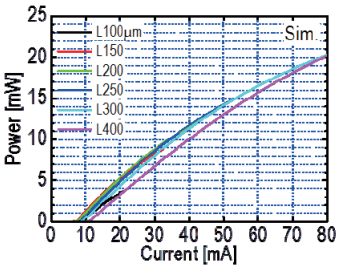


**Fig. 3** Calculated L-I characteristics of DFB laser.

for the LD and SOA ($I_{active}$) for the AXEL at the same value. We also set the sum of the LD and SOA lengths at 400 $\mu$m to investigate the tendency at the near value of the carrier density for the LD and SOA sections previously reported in Ref. [10]. As shown in Fig. 2, we changed the ratio of the length, and this changed the ratio of the current. When we fabricate the LD and SOA using the same MQW structure, the current is automatically divided according to their lengths [12].

Next, we calculated the light-current (L-I) characteristics for the LD section by using LASTIP (Crosslight Inc.) [16]. To calculate the output power of a DFB laser, we calculate the output power of a 300-$\mu$m-long FP laser with a mirror loss of 40 cm$^{-1}$. We estimate that the L-I curve of the FP laser with the different lengths by using the assumption of the same mirror loss. We estimate the output power of the DFB laser is 1.8 times larger than that of the FP laser with the anti-reflection and high reflection coated facets. In this estimation, a grating coupling coefficient ($\kappa$) is changed as the cavity length changes. We used the $\kappa$ value of 60 cm$^{-1}$ for the 200-$\mu$m DFB laser. Figure 3 shows the calculated output power from a DFB laser whose cavity length ranges from 100 to 400 $\mu$m. From the assumption in Fig. 2, the allocated $I_{LD}$ values for 100, 150, 250, and 300 $\mu$m LDs are 20, 30, 50, and 60 mA, respectively. As indicated in Fig. 3, the calculated output powers for 100, 150, 250, and 300 $\mu$m LDs are 5.4, 9.1, 11.5, and 12 dBm, respectively. This means that the output power is greatly reduced when the cavity length is reduced to 100 from 150 $\mu$m. This is caused by the reduced gain from a small active volume, and as the cavity becomes short, it will be difficult to overcome a threshold gain.

The modulated output power ($P_{avg}$) [dBm] of the AXEL can be expressed by

$$P_{avg} = P_{LD} - \alpha_{EA} + g_{SOA} \tag{1}$$

when $P_{LD}$ [dBm] is the LD output power, $\alpha_{EA}$ [dB] is the optical loss of the EAM, and $g_{SOA}$ [dB] is the SOA gain. We can estimate $P_{LD}$ from Fig. 3 for the various LD lengths. The $\alpha_{EA}$ value is set at roughly 7 dB, which is a typical value when the bias is applied to the EAM.

The SOA gain is also calculated with the help of a rate equation. The calculation method and the parameter values are provided in Ref. [10]. Figure 4 shows the SOA length, and the dependence of the calculated gain versus the optical input power on the SOA injection current. From these calculated results, we can estimate the way in which the extinction ratio is affected by the SOA gain. When the LD and SOA lengths are 300 and 100 $\mu$m, respectively, the calculated output power from the LD is 12 dBm and the estimated optical input into the SOA section is 5 dBm, because the $\alpha_{EA}$ is set at 7 dB. If the dynamic extinction ratio (*DER*) from the EAM is 8 dB and the "1" and "0" levels of the eye diagram input into the SOA are 9 and 1 dBm, respectively, with a center power of 5 dBm, the calculated gain of the 100-$\mu$m SOA for each level is 2.3 and 2.8 dB. This means the *DER* of the eye diagram from the EAM is slightly reduced when the modulated signal propagates in the SOA. As shown in Fig. 4, when designing the AXEL it is important to design an input power to the SOA that can provide a flat gain at both the "1" and "0" levels.

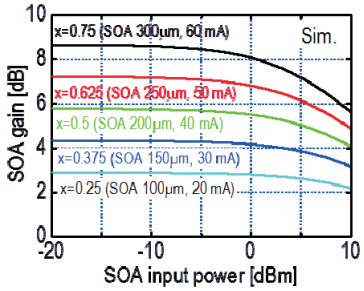


**Fig. 4** SOA length, and dependence of calculated gain versus optical input power on SOA injection current.

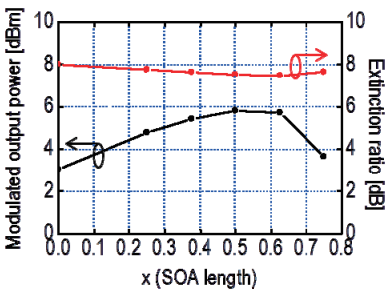


**Fig. 5** Calculated modulated output power and extinction ratio as SOA length parameter.

Figure 5 summarizes the calculated modulated output power emitted from the SOA. The modulated output power is estimated to be 3-dB smaller than the "1" level output power. The extinction ratio is also estimated under the assumption that the extinction ratio of the eye diagram from the EAM is 8 dB. The output power from the SOA increases as the SOA length increases. But too long an SOA will result in a reduction in output power of the LD section as described in Fig. 3. On the other hand, the extinction ratio decreases slightly as the SOA length increases. This is caused by the gain saturation of the SOA section as described in Fig. 4. The key to designing the AXEL is to balance the optical power of the LD and the SOA gain while maintaining the extinction ratio.

Table 1 summarizes the qualitative considerations when designing the AXEL. As the LD becomes shorter, it becomes difficult for the LD to provide a sufficient gain to overcome a threshold gain, and the reduced output power

from the LD becomes larger than the gain increase of the SOA. On the other hand, as the SOA becomes shorter, the SOA gain decreases but the output power of the LD increases. The key is to balance the LD and SOA lengths while tuning the reduced optical output power from the LD and the SOA gain. In addition, we need to take account of the pattern effect of the SOA section. The pattern effect can be suppressed by increasing the current of the SOA section [10]. The pattern effect influences the clearness of the eye diagram, and it is evaluated in terms of the bit error rate. For this reason, we need to confirm the effectiveness of the SOA by measuring the BER characteristics.

In this work, we set the LD and SOA lengths at 300 and 50 $\mu$m, respectively, to balance the pattern effect and SOA gain. We already have experimental data showing that the pattern effect is suppressed as $I_{\mathrm{SOA}}$ increases [11]. The other length ratio between the LD and SOA needs to be investigated to determine whether or not error-free operation can be obtained for the transmission after an appropriate distance.

Before measuring the characteristics of the designed AXEL, we estimated the actual current for the LD and SOA sections, because we cannot change the current value for these sections independently for the AXEL. $I_{\mathrm{LD}}$ and $I_{\mathrm{SOA}}$ can be estimated by

$$I_{active} = I_{LD} + I_{SOA} \tag{2}$$

$$I_{LD} = \frac{L_{LD}}{L_{LD} + L_{SOA}} \times I_{active} \tag{3}$$

$$I_{SOA} = \frac{L_{SOA}}{L_{LD} + L_{SOA}} \times I_{active} \tag{4}$$

where $I_{\mathrm{active}}$ is the injection current to the total active layer, and $L_{\mathrm{LD}}$ and $L_{\mathrm{SOA}}$ are the LD and SOA lengths, respectively. To estimate the actual current, we used an AXEL whose electrical input port was not connected. By using the device, we injected current only into the LD section and measured the photocurrent of the EAM with an EAM bias voltage of ($V_{\mathrm{EA}}$) −2.4 V. Next, we electrically connected the LD and SOA sections, and injected current and measured the difference from the previously measured value. With this method, we estimated the relation between the $I_{\mathrm{active}}$ value and $I_{\mathrm{LD}}$ and $I_{\mathrm{SOA}}$. Figure 6 shows measured relation between the $I_{\mathrm{active}}$ value and $I_{\mathrm{LD}}$ and $I_{\mathrm{SOA}}$. As shown in the figure, the current is actually divided almost according to the $L_{\mathrm{LD}}$ and $L_{\mathrm{SOA}}$ ratio corresponding to Eqs. (2), (3), and (4).

**Table 1** Qualitative aspects of AXEL.

| | Long LD + short SOA | Short LD + long SOA |
|---|---|---|
| Pros. | Small pattern effect<br>Large output power of LD | Small optical input to EAM<br>=Small $P$ of EAM<br>Large SOA gain |
| Cons. | Large optical input to EAM<br>=Large $P$ of EAM<br>Small SOA gain | Small output power of LD<br>Large pattern effect |

$P$: Power consumption.

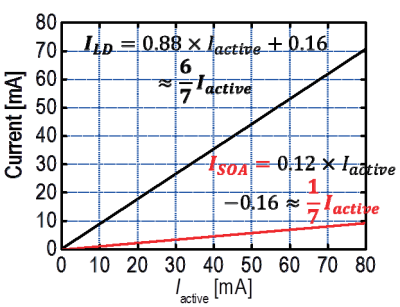


**Fig. 6** Estimated $I_{\mathrm{LD}}$ and $I_{\mathrm{SOA}}$ versus $I_{\mathrm{active}}$.

## 4. Device Characteristics

We fabricated an AXEL using the design methodology described above. Some of the basic structure has already been reported [10]. In addition, the electrical input ports of the LD and SOA sections are connected, and therefore the voltage for these sections automatically becomes the same for the AXEL. In this paper, the designed LD length ($L_{\mathrm{LD}}$) and SOA length ($L_{\mathrm{SOA}}$) are 300 and 50 $\mu$m, respectively, to balance the output power of the LD and the SOA gain while suppressing the pattern effect of the SOA section.

Figure 7 shows the light-current (L-I) characteristics of the EADFB laser and the AXEL at 50°C. The EA section is in an open circuit condition. The estimated optical fiber coupling loss is about 1.5 dB. As shown in the figure, the threshold current of the AXEL is larger than that of the EADFB laser because the AXEL needs additional current to compensate for the SOA loss, in other words, to make the SOA transparent. But when the current is increased, the efficiency of the current to optical power ratio of the AXEL is much larger than that of the EADFB laser. This result indicates that we can expect the AXEL to exhibit more energy efficient operation than the EADFB laser at an $I_{\mathrm{active}}$ of 80 mA.

Figure 8 shows the static extinction characteristics of the EADFB laser and AXEL at 50°C. The emitted optical output power from the EADFB laser or AXEL was measured when the $V_{\mathrm{EA}}$ was changed. As shown in the figure, when $I_{\mathrm{LD}}$ and $I_{\mathrm{active}}$ were both 80 mA, the optical output power of the AXEL was larger than that of the EADFB laser at $V_{\mathrm{EA}}$ values of 0 to −3 V. From this result, we estimated the extinction ratio of an eye diagram. If $V_{\mathrm{EA}}$ is −2.0 V, and the modulation voltage swing ($V_{\mathrm{pp}}$) is 2.0 V, the bias volt-

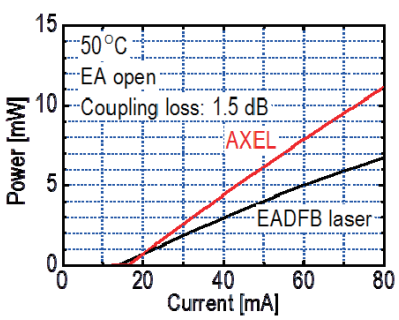


**Fig. 7** L-I characteristics of EADFB laser and AXEL at 50°C.

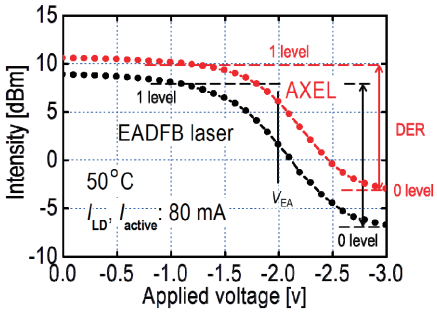


**Fig. 8** Static extinction characteristics of EADFB laser and AXEL.

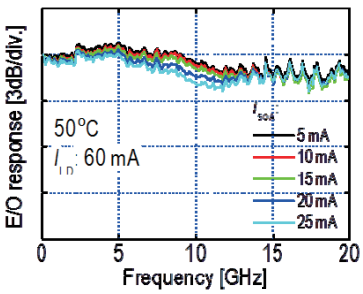


**Fig. 9** Measured E/O response of EADFB laser integrated with SOA.

age for the "1" and "0" eye diagram levels are −1 and −3 V, respectively. We can estimate the *DER* by calculating the difference between the optical output powers with $V_{EA}$ values of −1 and −3 V. As shown in Fig. 8, both the "1" and "0" levels of the eye diagram are amplified for the AXEL, and this means that the extinction ratio is maintained when the gain saturation of the SOA section is effectively suppressed.

To investigate the influence of the SOA on the electrical to optical (E/O) bandwidth, we measured the small signal E/O response of the EADFB laser integrated with an SOA. Figure 9 shows the E/O response of the EADFB laser with an SOA whose $I_{LD}$ was 60 mA. The current to the SOA section was changed from 5 to 25 mA. This condition is similar to the transmission experimental condition that is described later. In the transmission experiment, we assumed that the injected currents for LD and SOA sections for a 300-$\mu$m LD and a 50-$\mu$m SOA were 69 and 11 mA, respectively, when $I_{active}$ was 80 mA. Figure 9 clearly indicates that the AXEL has a large current tolerance as regards the 3-dB-down frequency bandwidth ($f_{3\,dB}$). Generally, the carrier life time is about 100 ps, which corresponds to about 10 GHz. If the carrier density in the SOA is sufficient, the current dependence of the frequency response will not be observed. But if the carrier density is not enough, the carrier will recover with time of 100 ps, and the frequency response shows some difference. As shown in Fig. 9, the current dependence of the frequency response is small. In this work, the SOA length is designed to 50 $\mu$m, and this design can provide the SOA with the sufficient current density. Thanks to the ridge structure and InGaAlAs core layer of the EAM, an $f_{3\,dB}$ of over 20 GHz was obtained with an SOA current of 5 to 25 mA. This value is sufficient for 10-Gbit/s operation.

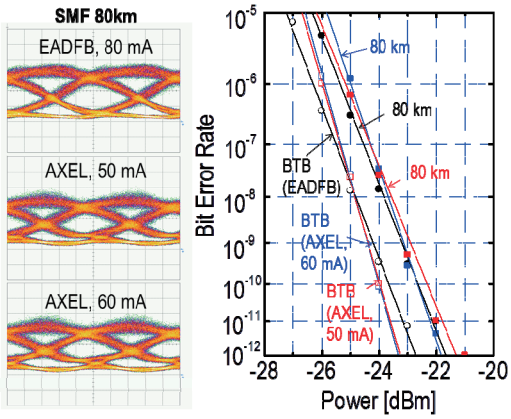


**Fig. 10** Eye diagrams and BER characteristics of EADFB laser and AXEL for 80-km SMF transmission.

**Table 2** Typical characteristics of EADFB laser and AXEL at 50°C.

| | $L_{LD}$ [μm] | $L_{SOA}$ [μm] | $I_{LD}$, $I_{active}$ [mA] | $V_{LD}$, $V_{active}$ [V] | $I_{EA}$ [mA] | $V_{EA}$ [V] | $P$ [mW] | $P_{avg}$ [dBm] |
|---|---|---|---|---|---|---|---|---|
| EADFB | 300 | - | 80 | 1.4 | -19 | -2.0 | 150 | 4.1 |
| | 300 | - | 80 | 1.4 | -22 | -2.4 | 170 | 1.7 |
| AXEL | 300 | 50 | 50 | 1.1 | -8.7 | -2.0 | 70 | 4.7 |
| | 300 | 50 | 60 | 1.2 | -11 | -2.0 | 90 | 5.7 |
| | 300 | 50 | 70 | 1.3 | -14 | -2.0 | 120 | 6.4 |
| | 300 | 50 | 80 | 1.3 | -17 | -2.0 | 140 | 6.9 |
| AXEL | 300 | 50 | 50 | 1.1 | -10 | -2.4 | 80 | 3.4 |
| | 300 | 50 | 60 | 1.2 | -14 | -2.4 | 110 | 4.1 |
| | 300 | 50 | 70 | 1.3 | -17 | -2.4 | 130 | 4.7 |
| | 300 | 50 | 80 | 1.3 | -21 | -2.4 | 160 | 5.1 |

$P$: Sum of power consumption of DFB, SOA and EA sections.
Power consumption of EA section calculated as $V_{EA} \times I_{EA}$.
$P_{avg}$: Modulated output power.

Because 1.55-$\mu$m EADFB lasers are widely used for 80-km SMF transmission applications, we compared the transmission characteristics of an EADFB laser with that of an AXEL. We set the operating temperature and the $V_{EA}$ at 50°C and −2.0 V, respectively. We used a 9.95-Gbit/s, non-return-zero (NRZ), pseudorandom binary sequence (PRBS) of $2^{31} - 1$. The $V_{pp}$ was set at −2.0 V. Figure 10 shows the eye diagrams after an 80-km SMF transmission and the bit-error-rate (BER) characteristics for the EADFB laser and AXEL. In this experiment, the injection current for the AXEL is reduced from 80 to 50 mA, while the BER is maintained to be similar value of the EADFB laser. As seen in the figure, there was no large difference for the BER characteristics between the EADFB laser with an $I_{LD}$ of 80 mA and an AXEL with an $I_{active}$ of 50 mA. In this case, the power consumption of the AXEL was about 70 mW while that of the EADFB laser was about 150 mW, as shown later in Table 2. A 50% reduction in power consumption was realized with the AXEL for the same transmission distance of 80 km.

Figure 11 shows eye diagrams and BER characteristics for the EADFB laser and AXEL at 50°C. $V_{EA}$ was set

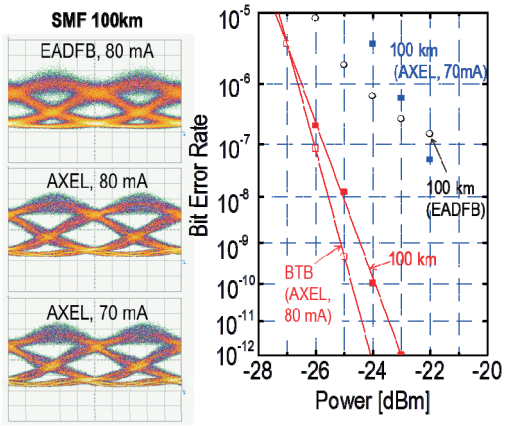


**Fig. 11** Eye diagrams and BER characteristics of EADFB laser and AXEL for 100-km SMF transmission.

at −2.4 V to investigate the upper limit of the transmission distance. A clear eye diagram after a 100-km SMF transmission was obtained with the AXEL when $I_{active}$ was 80 mA. On the other hand, the eye diagram of the EADFB laser after transmission through a 100-km SMF had deteriorated with the same $I_{LD}$. We consider this was caused by the chirp compensation that was required due to the SOA section [9]–[12]. The transmission distance of the AXEL can be extended to 100 km.

Table 2 shows the typical EADFB laser and AXEL characteristics at 50°C. When we compared an EADFB laser whose $V_{EA}$ was −2.0 V with an AXEL whose $I_{active}$ and $V_{EA}$ were 50 mA and −2.0 V, respectively, we found that the power consumption could be roughly halved. In this case, an 80 km transmission through SMF could be obtained for both devices. The $P_{avg}$ for the AXEL is larger than that of the EADFB laser. To evaluate the upper limit of the transmission distance, we reduced $V_{EA}$ from −2.0 to −2.4 V. In this case, the $P_{avg}$ decreased due to the increased loss of the EA section. When $I_{LD}$ and $I_{active}$ were both 80 mA, the $P_{avg}$ of the AXEL was 3.4 dB larger than that of the EADFB laser. As shown in Fig. 11, a 100 km transmission through SMF was only obtained with the AXEL thanks to its large output power. As shown in Table 2, we can extend the transmission distance by changing the $V_{EA}$ from −2.0 to −2.4 V. This is caused by the K-K relation that inevitably increases the loss of the EA section with the improved chirp parameter. AXEL can ease this limitation, because this concept can improve the current efficiency to optical power ratio. These results indicate that the AXEL can provide both an increased $P_{avg}$ and an extended transmission reach simultaneously without an additional electrical input port compared with a conventional EADFB laser. These results clearly indicate that the AXEL can replace the EADFB laser.

## 5. Conclusion

We have proposed a novel structure for an SOA assisted extended reach EADFB laser (AXEL) to overcome the limitation of the conventional EADFB laser. We explained the design methodology of the AXEL, which involved balancing the lengths of the LD and SOA. We then employed the design to fabricate a 1.55-$\mu$m AXEL by using InGaAlAs material for the LD, EA, and SOA core layers. With this AXEL, we roughly halved the power consumption and extended the transmission distance by 20 km at a signaling rate of 10 Gbit/s. We were able to operate the AXEL using the same electrical input port for the LD and SOA sections, and therefore no additional electrical input port was required. These results indicate that the AXEL can replace the EADFB laser.

## Acknowledgments

We thank Prof. Hiroshi Yasaka of the Research Institute of Electrical Communication, Tohoku University for his valuable advice. We also thank Dr. Takuo Hirono of NTT Electronics for the fruitful discussion about the simulation of the LD characteristics and Ms. Marie-Aline Mattelin of Ghent University in Belgium, for her support in measuring the device characteristics.

### References

[1] http://www.ieeee802.org/3/ba/
[2] http://www.ieeee802.org/3/bs/
[3] S. Makino, H. Hayashi, K. Shinoda, T. Kitatani, T. Shiota, S. Tanaka, M. Aoki, K. Naoe, N. Sasada, S. Yamauchi, M. Shishikura, T. Hatano, N. Morohashi, and H. Inoue, "Uncooled CWDM 25-Gbps EA/DFB lasers for cost-effective 100-Gbps Ethernet transceiver over 10-km SMF transmission," in Proc. OFC, PDP1, 2008.
[4] T. Saito, T. Yamatoya, Y. Morita, E. Ishimura, C. Watatani, T. Aoyagi, and T. Ishikawa, "Clear eye opening 1.3 $\mu$m-25/43 Gbps EML with novel tensile-strained asymmetric QW absorption layer," in Proc. ECOC, 8.1.3, 2008.
[5] K. Takada, M. Matsuda, S. Okumura, M. Ekawa, and T. Yamamoto, "Low-drive-current 10-Gb/s operation of AlGaInAs buried-heterostructure $\lambda$/4-shifted DFB lasers," in Proc. ECOC, Mo.3.4.4, 2006.
[6] T. Tatsumi, K. Tanaka, S. Sawada, H. Fujita, T. Abe, "1.3 $\mu$m, 56-Gbit/s EML Module target to 400GbE," in Proc. OFC, OTh3F4, 2012.
[7] W. Kobayashi, M. Arai, T. Yamanaka, N. Fujiwara, T. Fujisawa, T. Tadokoro, K. Tsuzuki, Y. Kondo, and F. Kano, "Design and Fabrication of 10-/40-Gbit/s, Uncooled Electroabsorption Modulator Integrated DFB Laser with Butt-Joint Structure," J. Lightwave Technol., vol.28, no.1, pp.164–171, 2010.
[8] H. Kim, S.K. Kim, H. Lee, S. Hwang, and Y. Oh, "Novel way to improve the dispersion-limited transmission distance of electroabsorption modulated lasers," IEEE Photon. Technol. Lett., vol.18, no.8, pp.947–949, 2006.
[9] T. Watanabe, N. Sakaida, H. Yasaka, F. Kano, and M. Koga, "Transmission performance of chirp-controlled signal by using semiconductor optical amplifier," J. Lightwave Technol., vol.18, no.8, pp.1069–1077, 2000.
[10] W. Kobayashi, M. Arai, T. Fujisawa, T. Sato, T. Ito, K. Hasebe, S. Kanazawa, Y. Ueda, T. Yamanaka, and H. Sanjoh, "Novel approach for chirp and output power compensation applied to a 40-Gbit/s EADFB laser integrated with a short SOA," Optics Express, vol.23, no.7, pp.9533–9542, 2015.
[11] W. Kobayashi, N. Fujiwara, K. Hasebe, S. Kanazawa, H. Sanjoh, and M. Itoh, "Recent progress on intensity and chirp compensation of EADFB laser realized by SOA integration," SPIE Photonics Eu-

rope 2016, 98921A (invited), Brussels, Belgium, 2016.
[12] W. Kobayashi, N. Fujiwara, T. Shindo, S. Kanazawa, K. Hasebe, H. Ishii, and M. Itoh, "Ultra low power consumption operation of SOA assisted extended reach EADFB laser (AXEL)," 21st Opto-Electronics and Communications Conference (OECC2016), WD3-2, Niigata, Japan, July 2016.
[13] W. Kobayashi, Japan patent JP5823920B (16, October, 2015)
[14] T. Shindo, W. Kobayashi, N. Fujiwara, Y. Ohiso, K. Hasebe, H. Ishii, and M. Itoh, "High modulated output power of +9.0 dBm transmitted over 80 km with L-band SOA assisted extended reach EADFB laser (AXEL)," 25th International Semiconductor Laser Conference (ISLC2016), TuC4, Kobe, Japan, September, 2016.
[15] K. Hasebe, W. Kobayashi, N. Fujiwara, T. Shindo, T. Yoshimatsu, S. Kanazawa, T. Ohno, H. Sanjoh, Y. Ohiso, H. Ishii, Y. Sone, and H. Matsuzaki, "28-Gbit/s 80-km transmission using SOA-assisted extended-reach EADFB laser (AXEL)," in Proc. OFC, accepted for publication, 2017.
[16] http://crosslight.com/

**Wataru Kobayashi** received B.S. and M.E. degrees in applied physics, and a Dr. Eng. degree in nano-science and nano-engineering from Waseda University, Tokyo, Japan, in 2003, 2005 and 2011, respectively. In 2005, he joined NTT Photonics Laboratories. He is now with NTT Device Technology Laboratories, Atsugi, Kanagawa, Japan. His research interests include the development of optical semiconductor devices. He is a member of Japan Society of Applied Physics (JSAP) and the Institute of Electronics, Information, and Communication Engineers (IEICE).

**Naoki Fujiwara** was born in Tokyo, Japan, in 1977. He received the B.E. and M.E. and Ph.D. degrees in electrical engineering from Waseda University, Tokyo, in 1999, 2001, and 2009 respectively. In 2001, he joined the Nippon Telegraph and Telephone (NTT) Photonics Laboratories (now NTT Device Innovation Center), NTT Corporation, Kanagawa, Japan. Since then, he has been engaged in developmental research on semiconductor lasers and integrated devices for optical communications systems. Dr. Fujiwara is a member of the Institute of Electronics, Information and Communication Engineers (IEICE) and the IEEE/Photonics Society.

**Takahiko Shindo** received his B.E., M.E., and Ph.D. degrees in Electrical and Electronic Engineering from Tokyo Institute of Technology, Japan, in 2008, 2010, and 2012, respectively. He received a research fellowship for young scientists from the Japan Society for the Promotion of Science for the years 2010 to 2012. After receiving the Ph. D. degree in 2012, he was working as a Research fellow at the Japan Society for the Promotion of Science, Japan. In April 2013, he joined Nippon Telegraph and Telephone (NTT) Photonics Laboratories (now NTT Device Technology Laboratories), NTT corporation, Atsugi-shi, Japan. He has been engaged in research on optical semiconductor devices. Dr Shindo is a member of the IEEE Photonics society, the Japan Society of Applied Physics, and the Institute of Electronics, Information and Communication Engineers of Japan.

**Yoshitaka Ohiso** received the B.S. M.S. and Ph.D. degrees in electrical engineering from Keio University, Yokohama, Japan in 1989, 1991, and 2003, respectively. Since joining the NTT laboratories, Kanagawa, Japan in 1991, he has been engaged in the research and development of optical semiconductor devices such as VCSEL, optical filter and optical modulator of EA and MZM. He also has been engaged in epitaxial growth of III-V compound semiconductors by MOCVD. Dr. Ohiso is a member of Japan Society of Applied Physics and the Institute of Electronics Information and Communication Engineers of Japan.

**Shigeru Kanazawa** was born in Kobe, Japan, in 1982. He received B.E., M.E. and Ph.D. degrees in electronic engineering from the Tokyo Institute of Technology, Tokyo, Japan, in 2005, 2007 and 2016, respectively. In April 2007, he joined Nippon Telegraph and Telephone (NTT) Photonics Laboratories (now NTT Device Innovation Center), Atsugi, Kanagawa, Japan. He is engaged in the research and development of optical semiconductor devices and integrated devices for optical communications systems. Dr. Kanazawa is a senior member of IEEE/Photonics Society and a member of the Japan Society of Applied Physics (JSAP) and the Institute of Electronics, Information and Communication Engineers of Japan.

**Hiroyuki Ishii** was born in Chiba, Japan, in 1966. He received B.E., M.E. and Ph.D. degrees in electronics and communication engineering from Waseda University, Tokyo, Japan, in 1988, 1990 and 1999 respectively. In 1990 he joined NTT Opto-electronics Laboratories (now NTT Device Technology Laboratories), Kanagawa, Japan. Since then, he has been engaged in developmental research on semiconductor lasers and integrated devices for optical communications systems. Dr. Ishii is a member of the Japan Society of Applied Physics (JSAP), the Institute of Electronics, Information and Communication Engineers (IEICE), and the IEEE/Photonics Society.

**Koichi Hasebe** received an M.E. and Ph.D. in electronics and applied physics from Tokyo Institute of Technology in 2005 and 2008. He received a research fellowship for young scientists from the Japan Society for the Promotion of Science for the years 2006 to 2009. In 2008, he was a postdoctoral fellow and visiting researcher at Tokyo Institute of Technology and the University of California, Berkeley, USA. He has been with NTT Photonics Laboratories since 2009. His current research interests include next-generation access systems, InP photonic functional devices, and nano-microcavity semiconductor lasers. He is a member of the IEICE and Optical Society of America (OSA).

**Hideaki Matsuzaki** was born in Osaka, Japan, in 1971. He received the B.S. and M.S. degrees in physics from Kyoto University, Kyoto, Japan, in 1993 and 1995, respectively. He joined Nippon Telegraph and Telephone Corporation (NTT)'s Atsugi Electrical Communications Laboratories in 1995. He is currently a Senior Research Engineer Supervisor with NTT Device Technology Laboratories, Kanagawa, Japan. He is a member of the IEEE, and the Institute of Electronics, Information, and Communication Engineers (IEICE) of Japan.

**Mikitaka Itoh** was born in Aichi, Japan, on October 26, 1968. He received the B.E., M.E., and Ph.D. degrees from Hokkaido University, Japan, in 1991, 1993 and 1996, respectively. In 1996, he joined Nippon Telegraph and Telephone (NTT) Interdisciplinary Research Laboratories (now NTT Device Technology Laboratories, Atsugi, Kanagawa, Japan). He is engaged in the research and development of silica-based planar lightwave circuits (PLCs) and semiconductor devices for optical communication systems. Dr. Itoh is a Member of IEEE Photonics Society, the Institute of Electronics, Information and Communication Engineers of Japan, and the Japan Society of Applied Physics (JSAP).